LETTER TO THE EDITOR

Prediction of the in-gap states above the top of the valence band in undoped insulating cuprates due to the spin-polaron effect

INSTITUTE OF PHYSICS PUBLISHING JOURNAL OF PHYSICS: CONDENSED MATTER

J. Phys.: Condens. Matter **16** (2004) L93–L100 PII: S0953-8984(04)73991-0

LETTER TO THE EDITOR

Prediction of the in-gap states above the top of the valence band in undoped insulating cuprates due to the spin-polaron effect

Sergei G Ovchinnikov, Alexey A Borisov, Vladimir A Gavrichkov and Maxim M Korshunov[1]

L V Kirensky Institute of Physics, Siberian Branch of the Russian Academy of Science, Krasnoyarsk, 660036, Russia

E-mail: mkor@iph.krasn.ru

Received 5 January 2004
Published 13 February 2004
Online at stacks.iop.org/JPhysCM/16/L93 (DOI: 10.1088/0953-8984/16/8/L04)

Abstract

In the framework of the generalized tight binding method we have calculated the quasiparticle band structure and the spectral functions of the undoped cuprates such as La_2CuO_4, $Sr_2CuO_2Cl_2$ etc. Due to spin fluctuations the in-gap state appears above the top of the valence band in the undoped antiferromagnetic insulator similar to in-gap states induced by hole doping. In the ARPES experiments the in-gap states can be detected as weak low energy satellites.

1. Introduction

The key issue to understand the nature of high temperature superconductivity in the cuprates is the evolution of the electronic structure from an antiferromagnetic insulator to a superconductor with hole doping. The appearance of the in-gap states above the top of the valence band in slightly doped cuprates has been found experimentally [1–4]. In the metallic underdoped regime the ARPES measurements [5] reveal the concentration dependent band structure of Bi-2212. With improving ARPES resolution recently the formation of new quasiparticle states at the transition from insulator to metal in $La_{2-x}Sr_xCuO_4$ has been found [6, 7].

The formation of the in-gap states with doping has been obtained theoretically in the numerical studies of small clusters in the framework of the t–J model, Hubbard model, and the three-band p–d model [8–11]. The band structure calculations of the CuO_2 layer in the framework of the multiband p–d model by the generalized tight-binding (GTB) method [12] with account for strong electron correlations have revealed the unusual in-gap state at the top of the valence band with zero spectral weight for undoped insulators that acquire the dispersion and non-zero spectral weight with hole doping [13]. In all models of strongly correlated

[1] Author to whom any correspondence should be addressed.

electrons the hopping of holes in the antiferromagnetic background is renormalized by spin fluctuations. To clarify the origin of the in-gap state we have studied in this paper a spin-polaron effect both analytically in the framework of the t–t'–J model and numerically by the GTB method similar to [13]. We have found that the spin fluctuations as well as hole doping provide non-zero spectral weight and dispersion of the in-gap state—even without doping, the spin excitations that are present in the antiferromagnetic state due to the quantum spin fluctuations at all temperatures including $T = 0$ result in non-zero in-gap spectral weight and dispersion above the top of the valence band. This state can be detected by the ARPES measurement as a weak satellite at the low energy shoulder of the main peak. Moreover, the concentration of spin fluctuations $n_{\rm sf}$ increases with temperature, and we expect the growth of the in-gap spectral weight $\sim n_{\rm sf}$.

2. GTB method results

A dispersion equation of the GTB method for the quasiparticle band structure of the CuO_2 layer looks like [13]

$$\left\| (E - \Omega_m^{\rm A})\delta_{mn} - 2F_\sigma^{\rm A}(m) \sum_{\lambda\lambda'} \gamma^*_{\lambda\sigma}(m) T^{\rm AB}_{\lambda\lambda'}(\vec{k}) \gamma_{\lambda'\sigma}(n) \right\| = 0. \tag{1}$$

Here m is a quasiparticle band index given by a pair (p, q) of the initial and final multielectron configurations $E_p(n+1)$ and $E_q(n)$; $\Omega_m = E_p(n+1) - E_q(n)$ is a local excitation energy. The local excitation $|q\rangle \to |p\rangle$ is described by the Hubbard operator $X^{pq} = |p\rangle\langle q|$; filling factor $F(m) = \langle X^{pp}\rangle + \langle X^{qq}\rangle$. Two magnetic sublattices are denoted by indices A and B, and σ is a spin projection. The interatomic hopping is $T^{\rm AB}_{\lambda\lambda'}$, where the single-hole basis set λ includes five orbitals, copper $d(x^2–y^2)$, $d(3z^2–r^2)$, in-plane oxygen $p(x)$, $p(y)$ and apical oxygen $p(z)$; $\gamma_{\lambda\sigma}(m)$ is a parameter of a single-hole annihilation operator in terms of the Hubbard operators

$$a_{\lambda\sigma} = \sum_m \gamma_{\lambda\sigma}(m) X^m. \tag{2}$$

The local multielectron energies and parameters $\gamma_{\lambda\sigma}(m)$ are obtained after the exact diagonalization of the multiband p–d model Hamiltonian for the unit cell. In our case the unit cell is a CuO_2 cluster for La_2CuO_4 and CuO_4Cl_2 for $Sr_2CuO_2Cl_2$. A similar equation has been known for a long time for the non-degenerate Hubbard model as the Hubbard I solution and has been used recently to study magnetic properties of transition metals [14, 15].

The essential multielectron configurations for undoped cuprates are $d^{10}p^6$ (vacuum state $|0\rangle$ in a hole representation), single-hole configurations d^9p^6 and $d^{10}p^5$ and two-hole configurations d^8p^5, d^9p^5, $d^{10}p^4$ and $d^{10}p^5p^5$. The minimal energy in the single-hole sector of the Hilbert space has the b_{1g} molecular orbital, and in the two-hole sector the $^1A_{1g}$ singlet that besides the Zhang–Rice singlet contains several more local singlets. A staggered magnetic field splits b_{1g} levels by spin:

$$\varepsilon_{{\rm A}\sigma} = \varepsilon_1 - \sigma h, \qquad \varepsilon_{{\rm B}\sigma} = \varepsilon_1 + \sigma h. \tag{3}$$

The top of the valence band is given by the quasiparticles with $m = 1 : X^1_{\rm A} = |b_{1g,\uparrow}\rangle\langle {}^1A_{1g}|$ and $X^1_{\rm B} = |b_{1g,\downarrow}\rangle\langle {}^1A_{1g}|$, as there is usually spin degeneracy of the band in the antiferromagnetic state. The occupation numbers $n_p \equiv \langle X^{pp}\rangle$ are calculated self-consistently via the chemical potential equation. In the mean-field Hubbard I approximation the solution of this equation for the hole-doped cuprates with hole concentration $n_{\rm h} = 1 + x$ is given by

$$n_{1\uparrow} \equiv n_{{\rm A}\uparrow}(b_{1g}) = 1 - x, \qquad n_{1\downarrow} = 0, \qquad n_2 \equiv n({}^1A_{1g}) = x. \tag{4}$$

For the band $m = 1$ we get $F_{{\rm A}\uparrow}(1) = 1$ while for the band $m = 2$ with $X^2_{\rm A} = |b_{1g,\downarrow}\rangle\langle {}^1A_{1g}|$ the filling factor is $F_{{\rm A}\downarrow}(2) = x$. The quasiparticle spectral weight is proportional to the

filling factor, thus it is the band $m = 2$ that forms the in-gap state. In the limit $x \to 0$ its spectral weight is zero; when $x \neq 0$ this band acquires both dispersion and non-zero spectral weight. The corresponding concentration-dependent band structure has been obtained for $La_{2-x}Sr_xCuO_4$ in [13] and the chemical potential $\mu(x)$ dependence and the Fermi surface evolution with doping have been studied in [16].

To go beyond the mean-field Hubbard I approximation one has to calculate single-loop diagrams for the self-energy [17]. In the ferromagnetic or antiferromagnetic state the most important contribution is given by loops with spin-wave excitations [18] (a spin-polaron effect). According to [18], the main effect of the spin excitations is given by the spin-wave renormalization of the multielectron configuration's occupation numbers, so instead of (4) one gets

$$n_{1\uparrow} = (1-x)(1-n_{sf}), \qquad n_{1\downarrow} = (1-x)n_{sf}, \qquad n_2 = x, \tag{5}$$

where n_{sf} is the occupation of the spin-minority level and it determines the spin-fluctuation decrease of the sublattice magnetization

$$\langle S_A^z \rangle = (1-x)(1/2 - n_{sf}). \tag{6}$$

Concentration of the spin fluctuations (magnons) is equal to $2n_{sf}$.

Thus the filling factor for the valence band $F(1) = 1 - n_{sf}$, and for the in-gap states $F(2) = x + n_{sf}$. This means that the spin-polaron effect results in non-zero spectral weight of the in-gap states even for undoped cuprates La_2CuO_4 and $Sr_2CuO_2Cl_2$.

In [21] the value $n_{sf} = 0.2$ was obtained self-consistently in the effective quasi-two-dimensional Heisenberg antiferromagnetic model for a ratio typical in La_2CuO_4 of 10^{-5} of the interplane and intraplane exchange parameters. From the neutron diffraction studies of La_2CuO_4 [22] and $YBa_2Cu_3O_6$ [23] it is known that the value of magnetic moment on copper M_{Cu} is given by $M_{Cu} \approx 0.5\ \mu_B$ where μ_B is the Bohr magneton. There are two reasons for the M_{Cu} difference from the value $1.14\ \mu_B$ in Cu^{2+}, namely the zero-temperature quantum fluctuations and the covalent effects. Since each oxygen has two neighbouring coppers belonging to different magnetic sublattices the total moment on oxygen is equal to zero. But due to p–d hybridization the p states of oxygen are partially filled so these orbitals could carry non-zero magnetic moment M_O, while the total moment on oxygen will be equal to zero. Such space distribution of magnetic moment leads to a difference between the M_{Cu} experimentally observed and calculated from the simple Heisenberg model. Therefore, the value $n_{sf} = 0.2$ is overestimated. In order to take into account covalent effects and zero quantum fluctuations on equal footing we will write down the expression for M_{Cu}:

$$M_{Cu} = 2.28\ \mu_B \langle S_A^z \rangle u^2, \tag{7}$$

where zero quantum fluctuations are contained in $\langle S_A^z \rangle$ and covalent effects are described by the weight u^2 of the d^9p^6 configuration. The last quantity could be calculated in the framework of the GTB method and is given by $u^2 = 0.6061$. Using equations (7) and (6) it is possible to calculate n_{sf}, which for the experimentally observed $M_{Cu} = 0.5\ \mu_B$ is equal to $n_{sf} = 0.138$. In the present paper we will use this value of n_{sf}.

The quasiparticle band structure and the spectral functions for the undoped La_2CuO_4 with $n_{sf} = 0.138$ are given in figure 1. The band formed by hole hopping via the two-hole triplet $^3B_{1g}$ state lies at ≈ -1.4 eV and is not shown here (the physics of this state was discussed in detail in [13, 19]). The lowest band in figure 1 is the top of the valence band ($m = 1$) without spin fluctuations with a maximum at $k = (\pi/2, \pi/2)$. The upper band ($m = 2$) is formed by the dispersion of the in-gap states. Despite its width each state has a low spectral weight as seen in figure 1(b) and the total number of states in this in-gap band (without doping) is equal to n_{sf}. The appearance of such non-Fermi liquid states is the direct effect of strong electron

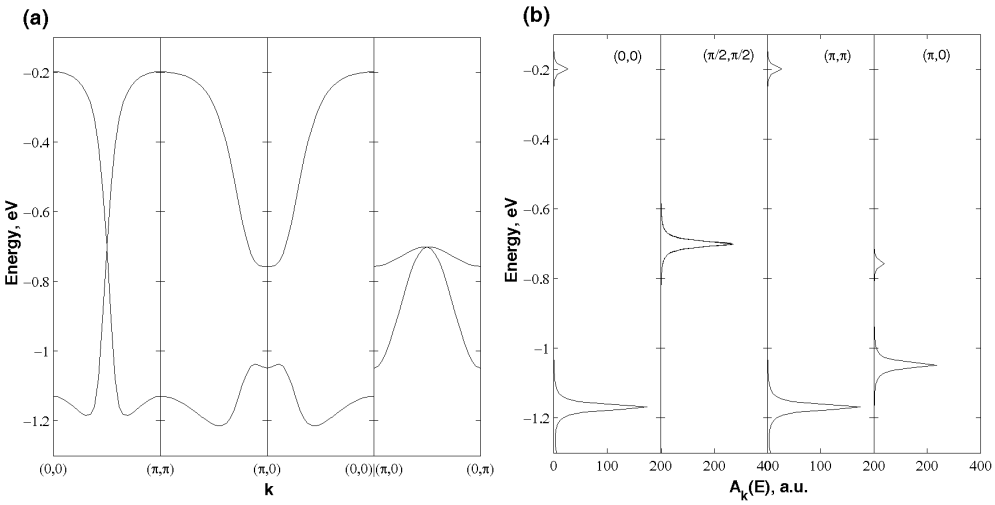

Figure 1. The quasiparticle band structure (a) and the spectral function (b) of the undoped La_2CuO_4 with a spin fluctuation $n_{sf} = 0.138$ calculated by the GTB method. The Fermi level is above all bands shown here.

correlations. The maximal spectral weight of the in-gap state is near the $(\pi, 0)$ point of the Brillouin zone (BZ). At the $(\pi/2, \pi/2)$ point the two bands are degenerate, and we cannot separate the contribution of the in-gap band to the spectral function $A_k(E)$.

3. t–t'–J model treatment

To clarify the properties of the in-gap band we study the spin-polaron effect in the t–t'–J model, which is an effective low energy model for the multiband p–d model [20], with the Hamiltonian

$$H_{t-J} = (\varepsilon_1 - \mu)\sum_{f,\sigma} X_f^{\sigma\sigma} + \sum_{\langle f,g\rangle,\sigma} t_{fg} X_f^{\sigma 0} X_g^{0\sigma} + \sum_{\langle f,g\rangle} J_{fg}(\mathbf{S}_f \mathbf{S}_g - \tfrac{1}{4} n_f n_g), \tag{8}$$

where $\mathbf{S}_f$ are spin operators and n_f are numbers of particle operators; t_{fg} and J_{fg} are the hopping and exchange integrals respectively. In the Hubbard I approximation it is easy to obtain in the undoped case the following intrasublattice and intersublattice Green functions ($f \in$ A, $g \in$ B):

$$\langle\langle X_f^{0\sigma} | X_{f'}^{\sigma 0}\rangle\rangle_E = \frac{2}{N}\sum_k G_{k\sigma}^{\mathrm{AA}}(E) \mathrm{e}^{\mathrm{i}\vec{k}(\vec{f}-\vec{f}')},$$

$$\langle\langle X_g^{0\sigma} | X_{f'}^{\sigma 0}\rangle\rangle_E = \frac{2}{N}\sum_k G_{k\sigma}^{\mathrm{BA}}(E) \mathrm{e}^{\mathrm{i}\vec{k}(\vec{g}-\vec{f}')}.$$

The matrix Green function in momentum space could be written as

$$\hat{G}_{k\sigma} = \begin{pmatrix} G_{k\sigma}^{\mathrm{AA}} & G_{k\sigma}^{\mathrm{AB}} \\ G_{k\sigma}^{\mathrm{BA}} & G_{k\sigma}^{\mathrm{BB}} \end{pmatrix} = \frac{1}{D}\begin{pmatrix} n_{\mathrm{A}\sigma}(E - \varepsilon_{k\sigma}^{\mathrm{B}}) & n_{\mathrm{A}\sigma} n_{\mathrm{B}\sigma} t_k^{\mathrm{B}} \\ n_{\mathrm{A}\sigma} n_{\mathrm{B}\sigma} t_k^{\mathrm{B}} & n_{\mathrm{B}\sigma}(E - \varepsilon_{k\sigma}^{\mathrm{A}}) \end{pmatrix}, \tag{9}$$

where $D = (E - E_{k\sigma}^{+})(E - E_{k\sigma}^{-})$ and $\varepsilon_{k\sigma}^{\alpha} = (\varepsilon_1 - \mu) - (J_0^{\mathrm{B}} - t_k^{\mathrm{A}}) n_{\alpha\sigma} - J_0^{\mathrm{A}} n_{\alpha\tilde{\sigma}}$, with $\alpha =$ A, B.

Here t_k^{B} and t_k^{A} (J_0^{B} and J_0^{A}) are the hoppings (exchanges) in momentum space between different and the same sublattices respectively. In the simple case of the next nearest neighbour approximation we have

$t_k^{\mathrm{B}} = 2t(\cos k_x + \cos k_y)$, $t_k^{\mathrm{A}} = 4t' \cos k_x \cos k_y$, $J_0^{\mathrm{B}} = 4J$, $J_0^{\mathrm{A}} = 4J'$,

with primed values corresponding to next nearest hoppings and exchanges. The occupation factors of the one-particle state with different spin projections are denoted by $n_{\mathrm{A}\sigma}$ and $n_{\mathrm{B}\sigma}$. In the mean field Hubbard I approximation $n_{\mathrm{A}\uparrow} = (1 - n_{\mathrm{sf}})$ and $n_{\mathrm{A}\downarrow} = 0$ at $T = 0$. Using the same arguments as in section 2, we go beyond the Hubbard I approximation by renormalization of the occupation numbers with spin fluctuations. For the undoped La_2CuO_4 this results in

$$n_{\mathrm{A}\uparrow} = (1 - n_{\mathrm{sf}}), \qquad n_{\mathrm{A}\downarrow} = n_{\mathrm{sf}}, \qquad n_{\mathrm{B}\sigma} = n_{\mathrm{A}\bar{\sigma}}. \tag{10}$$

The condition $D = 0$ gives two branches of the quasiparticle spectrum:

$$E_{k\uparrow}^{\pm} = \varepsilon_1 - \mu + \tfrac{1}{2}[t_k^{\mathrm{A}} - J_0^{\mathrm{B}} - J_0^{\mathrm{A}} \pm \beta_k] \tag{11}$$

where

$$\beta_k = \sqrt{(t_k^{\mathrm{A}} - J_0^{\mathrm{B}} + J_0^{\mathrm{A}})^2(1 - 2n_{\mathrm{sf}})^2 + 4(t_k^{\mathrm{B}})^2(1 - n_{\mathrm{sf}})n_{\mathrm{sf}}}.$$

If we set the concentration of the magnons to zero we immediately get one dispersionless state and one dispersive state with dispersion governed by intrasublattice hoppings:

$$E_{k\uparrow}^{+}|_{n_{\mathrm{sf}}=0} = \varepsilon_1 - \mu - J_0^{\mathrm{A}}, \qquad E_{k\uparrow}^{-}|_{n_{\mathrm{sf}}=0} = \varepsilon_1 - \mu + t_k^{\mathrm{A}} - J_0^{\mathrm{B}}. \tag{12}$$

If the values of intrasublattice hoppings and exchange are small then the difference between two energy levels is of order J:

$$\Delta E|_{n_{\mathrm{sf}}=0} = (E_{k\uparrow}^{+} - E_{k\uparrow}^{-})|_{n_{\mathrm{sf}}=0} \approx 4J. \tag{13}$$

In figure 2(a) the quasiparticle dispersions corresponding to equations (11) and (12) are shown. Parameters were taken from the effective low energy model [20] of the multiband p–d model and are given by $t = 0.587$, $t'/t = -0.085$, $J/|t| = 0.392$, $J'/|t| = 0.0004$ and $n_{\mathrm{sf}} = 0.138$.

The distance between two spectrum branches for non-zero concentration of the magnons is less than distance (13) for $n_{\mathrm{sf}} = 0$ by a factor proportional to $(1 - 2n_{\mathrm{sf}}) = 2\langle S^z \rangle$.

The lower quasiparticle branch for $n_{\mathrm{sf}} = 0.138$ (but not for $n_{\mathrm{sf}} = 0$!) clearly resembles the dispersion obtained in the self-consistent Born approximation [24] and the GTB method [13]. This proves that two different approaches to treat spin fluctuations lead to similar results.

Introducing the energy difference $\Delta E_k \equiv E_{k\uparrow}^{+} - E_{k\uparrow}^{-}$ we can write down spectral functions $A_{k\sigma}(E) = -\frac{1}{\pi} \operatorname{Im}[Sp\hat{G}_{k\sigma}]$ in the form

$$A_{k\uparrow}(E) = u_k^2 \delta(E - E_{k\uparrow}^{+}) + v_k^2 \delta(E - E_{k\uparrow}^{-}), \tag{14}$$

$$A_{k\downarrow}(E) = v_k^2 \delta(E - E_{k\downarrow}^{+}) + u_k^2 \delta(E - E_{k\downarrow}^{-}), \tag{15}$$

where

$$u_k^2 = \frac{1}{2} - (1 - 2n_{\mathrm{sf}})^2 \frac{(J_0^{\mathrm{B}} - J_0^{\mathrm{A}} - t_k^{\mathrm{A}})}{2\Delta E_k}, \qquad v_k^2 = 1 - u_k^2.$$

Obviously, for $n_{\mathrm{sf}} = 0$ the value $u_k^2 = 0$, $v_k^2 = 1$ and there will be the non-zero spectral function $A_{k\uparrow}(E) = \delta(E - E_{k\uparrow}^{-})$ corresponding to only one dispersive state (12). In figure 2(b) the spectral functions versus energy for different symmetric points in momentum space are shown. Comparison of spectral intensities in the case of the presence and absence of n_{sf} (solid and dash–dotted curves) indicates that the second satellite peak appears above the main peak at $(\pi/2, \pi/2)$ and $(\pi, 0)$ points. It is the satellite peak that represents the in-gap state. At the $(\pi/2, \pi/2)$ point the distance between two peaks is proportional to J (see equation (13)) but at the $(\pi, 0)$ point the distance is proportional to $|J + t'|$ (or, generally, $|J_0^{\mathrm{B}} - t_k^{\mathrm{A}}|$) and will also take place even at zero J. The last statement emphasizes the importance of next nearest

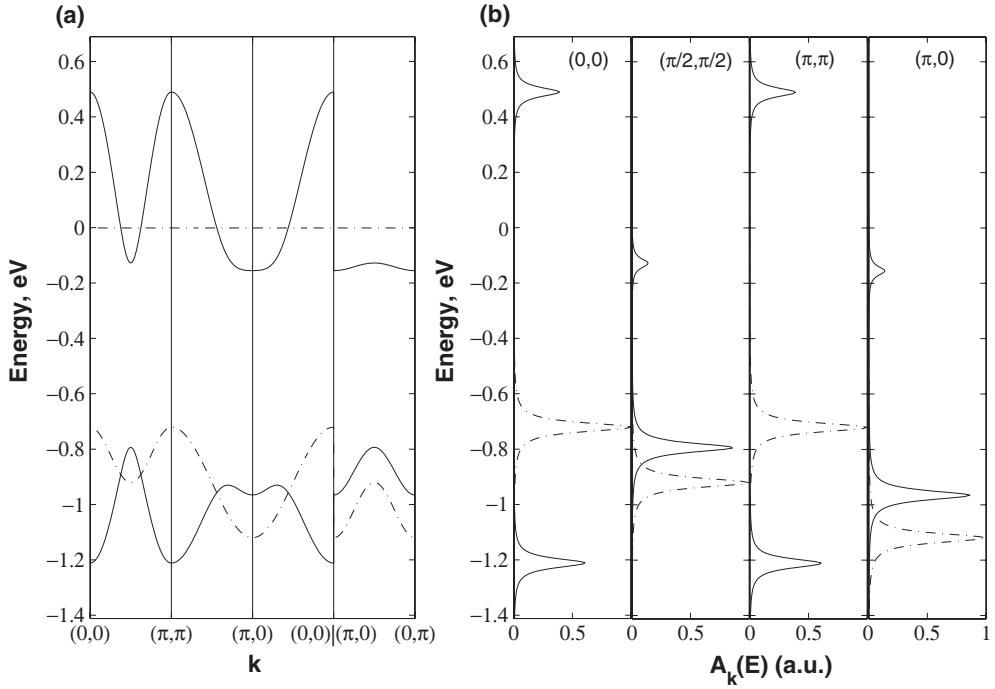

Figure 2. Quasiparticle dispersion (a) and spectral function peaks (b) in the t–t'–J model for $x = 0$ and $n_{\rm sf} = 0.138$ (solid curves), $n_{\rm sf} = 0$ (dot–dashed curves).

neighbour hoppings t' at low doping. Indeed, if one considers the t–J model with only nearest neighbour hoppings then the doped hole will not even be able to move without spin fluctuations ($n_{\rm sf} = 0$, see equation (12)) and at low $n_{\rm sf}$ the dispersion will be governed by the $(t_k^{\rm A} - J_0^{\rm B})$ term in equation (11) but not by nearest neighbour hopping $t_k^{\rm B}$. In the case of the t–J model with $t' = 0$ the quasiparticle spectrum (11) becomes

$$E_{k\uparrow}^{\pm}|_{t'=0} = \varepsilon_1 - \mu + 2J \pm 2\sqrt{J^2(1-2n_{\rm sf})^2 + t^2(\cos k_x + \cos k_y)^2(1-n_{\rm sf})n_{\rm sf}}. \tag{16}$$

One can easily see that the two branches of this spectrum have the same dispersion proportional to $(\cos k_x + \cos k_y)n_{\rm sf}$ and at $n_{\rm sf} = 0$ there will be two dispersionless states. So we conclude that the in-gap band forms even at zero t' but at low magnon concentration the dispersion of this band is governed exactly by intrasublattice hoppings (t', or, generally, $t_k^{\rm A}$).

Now we will discuss the higher-order corrections to previous results. Two main effects are expected: (i) quasiparticle decay and (ii) renormalization of the real part of the self-energy. The main change with introduction of finite quasiparticle lifetime will be broadening of spectral peaks. This effect is indirectly presented in figure 2(b) where the delta function peaks in the spectral function are artificially broadened by the Lorentzian. Still, there could be a strong energy and momentum dependence of the imaginary part of the self-energy, which analysis is far from the scope of the present paper. To analyse the renormalization of the real part of the self-energy we will use a more rigorous approximation—the generalized Hartree–Fock approximation [25]. In this approximation the equation of motion for operator $X_f^{0\sigma}$ is renormalized by two-site static correlation functions,

$$\mathrm{i}\frac{\mathrm{d}}{\mathrm{d}t}X_f^{0\sigma} = [(\varepsilon_1 - \mu) + M_{f\sigma}]X_f^{0\sigma} + \sum_g \tau_{fg,\sigma}X_g^{0\sigma}, \tag{17}$$

where $M_{f\sigma}$ and $\tau_{fg,\sigma}$ are the renormalized chemical potential (exchange integral) and hopping integrals respectively:

$$M_{f\sigma} = \sum_g t_{fg}\langle X_f^{0\bar{\sigma}} X_g^{\bar{\sigma}0}\rangle - \sum_g J_{fg}[\langle X_f^{00} X_g^{\bar{\sigma}\bar{\sigma}}\rangle + \langle X_f^{\sigma\bar{\sigma}} X_g^{\bar{\sigma}\sigma}\rangle - \langle X_f^{\sigma\sigma} X_g^{\bar{\sigma}\bar{\sigma}}\rangle],$$

$$\tau_{fg,\sigma} = t_{fg}[\langle X_f^{00} X_g^{00}\rangle + \langle X_f^{00} X_g^{\sigma\sigma}\rangle + \langle X_f^{\sigma\sigma} X_g^{00}\rangle + \langle X_f^{\sigma\sigma} X_g^{\sigma\sigma}\rangle + \langle X_f^{\bar{\sigma}\sigma} X_g^{\sigma\bar{\sigma}}\rangle] + J_{fg}\langle X_f^{0\bar{\sigma}} X_g^{\bar{\sigma}0}\rangle.$$

It is clear that equation (17) has the same linearized form as in the Hubbard I approximation but with renormalized chemical potential and hopping integrals. This means the qualitative results of the Hubbard I consideration will be the same but quantitatively they may change. Namely, due to renormalization of the exchange integral the distance between the in-gap and main spectral peaks will be shorter than expected from (13) and a concentration dependence of peak positions will appear due to both renormalizations. Meanwhile, the underlying physics of the in-gap state will be unchanged and its dispersion will be governed by spin fluctuations.

4. Conclusion

It is clear from the spectral function both in figures 1(b) and 2 (b) that there is a pseudogap between the in-gap band and the valence band; for the undoped cuprate both bands are occupied and the chemical potential lies above the in-gap band. With doping $\mu(x)$ is pinned to the in-gap state [16] up to optimal doping. The pseudogap is k-dependent. At the $(\pi/2, \pi/2)$ point of the BZ the value of the gap is given by $\Delta E(\pi/2, \pi/2) \sim J(1 - 2n_{\rm sf})$, while at the $(\pi, 0)$ point $\Delta E(\pi, 0) \sim |J + t'|(1 - 2n_{\rm sf})$. In the p–d model we have not considered the interband excitations between the lower and upper Hubbard bands (full filled valence band for electrons and empty conductivity band) forming the effective $J \sim t^2/U$; this means equation (1) and its solution were obtained in the $U \to \infty$ limit. In the t–J model we considered a finite value of U; that is why there is a difference in the spectral functions in figures 1 and 2. In the limit $U \to \infty$ ($J \to 0$) the mentioned difference disappears—we get $\Delta E(\pi/2, \pi/2) \to 0$ and $\Delta E(\pi, 0) \to |t'|(1 - 2n_{\rm sf})$, that corresponds to figure 1(b). At $J \neq 0$ there is the additional contribution to the pseudogap, and we may expect the in-gap satellite both at $(\pi/2, \pi/2)$ and $(\pi, 0)$ points of the BZ.

In conclusion, we have shown that the spin-polaron effect results in the formation of the in-gap band above the top of the valence band even in the undoped cuprates. Previously, the evidence for the in-gap states was found only in lightly doped $La_{2-x}Sr_xCuO_4$. Our results shows that these states should appear in all undoped antiferromagnetic cuprates, namely La_2CuO_4, $Sr_2CuO_2Cl_2$ and $Ca_2CuO_2Cl_2$. Although the appearance of the in-gap states is common for the high T_c substances with CuO_2 planes the experimental evidence for the in-gap states in cuprates such as $Bi_2Sr_2CaCu_2O_{8+\delta}$ and $YBa_2Cu_3O_{7-\delta}$ could be shaded by other stronger effects due to the more complicated structure of these compounds (non-stoichiometry, presence of oxygen chains in YBCO, etc). The spectral function of the in-gap states has the form of a small low energy satellite that can be detected by ARPES measurements. The most interesting for the ARPES studies are the $(\pi, 0)$ and $(\pi/2, \pi/2)$ points of the BZ. For the hole-doped cuprates there are two contributions to the in-gap spectral weight: the mean-field contribution is given by doping concentration x and the spin-fluctuation contribution is given by the magnon concentration $2n_{\rm sf}$. The latter is temperature dependent, resulting in increasing satellite intensity with temperature growth.

The authors are thankful to Yu A Izyumov and V I Anisimov for stimulating discussion. This work was supported by RFFI grant 03-02-16124, INTAS grant 01-0654, the Russian Academy of Science Programme 'Quantum macrophysics', the Joint Integration Programme of Ural and

Siberian Branches of RAS and the Siberian Branch of RAS (Lavrent'yev Contest for Young Scientists).

References

[1] Suzuki M 1989 *Phys. Rev.* B **39** 2312
[2] Uchida S *et al* 1991 *Phys. Rev.* B **43** 7942
[3] Fujimori A and Namatame N 1991 *Physica* C **185–189** 51
[4] Bazhenov A V, Gorbunov V A and Timofeev V E 1993 *JETP* **104** 3193
[5] Marshall D S *et al* 1996 *Phys. Rev. Lett.* **76** 4841
[6] Ino A *et al* 2000 *Phys. Rev.* B **62** 4137
[7] Yoshida T *et al* 2003 *Phys. Rev. Lett.* **91** 027001
[8] Stephan W and Horsh P 1991 *Phys. Rev. Lett.* **66** 2258
[9] Dagotto E *et al* 1991 *Phys. Rev. Lett.* **67** 1918
[10] Tohyama T and Maekawa S 1992 *Physica* C **191** 193
[11] Press R, Hanke W and von der Linden W 1995 *Phys. Rev. Lett.* **75** 1344
[12] Ovchinnikov S G and Sandalov I S 1989 *Physica* C **198** 607
[13] Gavrichkov V A *et al* 2000 *JETP* **91** 369
[14] Zaitsev R O 1997 *JETP Lett.* **65** 881
[15] Zaitsev R O 2000 *JETP Lett.* **72** 109
[16] Borisov A A, Gavrichkov V A and Ovchinnikov S G 2003 *JETP* **97** 773
[17] Zaitsev R O 1975 *JETP* **41** 100
[18] Podmarkov A N and Sandalov I S 1984 *JETP* **86** 146
[19] Gavrichkov V A, Ovchinnikov S G and Borisov A A 2001 *Phys. Rev.* B **64** 235124
[20] Korshunov M M and Ovchinnikov S G 2001 *Phys. Solid State* **43** 416
[21] Horsch P and von der Linden W 1988 *Z. Phys. B* **72** 181
[22] Vaknin D *et al* 1987 *Phys. Rev. Lett.* **58** 2802
[23] Tranquada J M *et al* 1988 *Phys. Rev.* B **38** 2477
[24] Nazarenko A *et al* 1995 *Phys. Rev.* B **51** 8676
[25] Tyablikov S V 1975 *Methods of Quantum Theory of Magnetism* 2nd edn (Moscow: Nauka)